ACS SENSORS

pubs.acs.org/acssensors

Article

Rapid Detection of Gram-Positive and -Negative Bacteria in Water Samples Using Mannan-Binding Lectin-Based Visual Biosensor

Mahdi Naseri, Maisha Maliha, Mostafa Dehghani, George P Simon, and Warren Batchelor*

Cite This: *ACS Sens.* 2022, 7, 951−959

Read Online

ACCESS | Metrics & More | Article Recommendations | Supporting Information

ABSTRACT: Waterborne bacterial infection is a health threat worldwide, making accurate and timely bacteria detection crucial to prevent waterborne disease outbreaks. Inspired by the intrinsic capability of mannan-binding lectin (MBL) in recognizing the pathogen-associated molecular patterns (PAMPs), a visual biosensor is developed here for the on-site detection of both Gram-positive and -negative bacteria. The biosensor was synthesized by immobilization of the MBL protein onto the blue carboxyl-functionalized polystyrene microparticles (PSM), which is then used in a two-step assay to detect bacterial cells in water samples. The first step involved a 20 min incubation following the MBL-PSM and calcium chloride solution addition to the samples. The second step was to add ethanol to the resultant blue mixture and observe the color change with the naked eye after 15 min. The biosensor had a binary (all-or-none) response, which in the presence of bacterial cells kept its blue color, while in their absence the color changed from blue to colorless. Testing the water samples spiked with four Gram-negative bacteria including *Acinetobacter baumannii*, *Escherichia coli*, *Klebsiella pneumoniae*, and *Pseudomonas aeruginosa* and two Gram-positive bacteria of *Enterococcus faecalis* and *Staphylococcus aureus* showed that the biosensor could detect all tested bacteria with a concentration as low as $10^{1.5}$ CFU/ml. The performance of biosensor using the water samples from a water treatment plant also confirmed its capability to detect the pathogens in real-life water samples without the need for instrumentation.

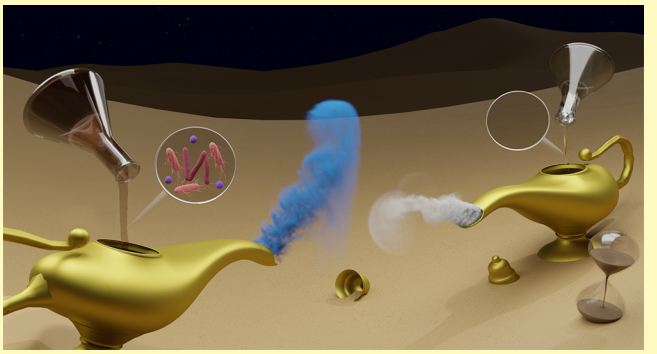

KEYWORDS: *Bacteria, Biosensor, Colorimetric, Mannan-binding lectin, Water*

Monitoring the microbiological safety of potable water is crucial to prevent outbreaks associated with waterborne pathogens.[1] These include bacteria, viruses, and parasites of which bacteria, due to their higher prevalence, are the most important in water quality surveillance.[2,3] The conventional methods for the detection of bacteria include plate count, nucleic acid, and immunological assays which require the transfer of samples to a laboratory and waiting for several hours to obtain the results.[3,4] Despite their high accuracy, a long waiting time made other technologies such as biosensors, which offer a rapid on-site detection, of high interest.[5]

Biosensors are often classified into electrochemical, optical, thermal, and mass-sensitive, depending on their signal transduction mechanism.[6] Visual biosensors are a subtype of colorimetric optical biosensors which upon recognizing the analyte transduce a colorimetric signal readable and interpretable by the naked eye.[2] Such visual biosensors capable of rapid detection of both Gram-positive and -negative bacteria in water samples have been introduced in recent years. Sun et al.[7] developed a biosensor that could detect live bacteria by measuring the presence of glucose in their environment. When the bacterial cells were absent, the biosensor showed a deep blue color, while in their presence it became colorless. Using this system, they could detect Gram-negative *Escherichia coli* (*E. coli*) and Gram-positive *Staphylococcus aureus* (*S. aureus*) with the reported detection limit of 10^3 CFU/mL in 20 min. In another study, Huang et al.[8] used 4-mercaptophenylboronic acid (4-MPBA)-functionalized gold nanoparticles which could change color from dark blue to red in the presence of bacteria in 20 min. This biosensor allowed the detection of Gram-negative *E. coli*, *Salmonella pullorum*, and Gram-positive *S. aureus*, *Enterococcus faecalis* (*E. faecalis*), and *Streptococcus mutans* with the detection limit of 10^3 CFU/mL. Recently, Du et al.[9] developed a gold nanoparticle-based biosensor that changed color from red to blue in the presence of bacteria in 5 min. The biosensor could detect Gram-negative *E. coli*, *Pseudomonas aeruginosa* (*P. aeruginosa*), *Salmonella typhimurium* (*S. typhimurium*), *Vibrio parahemolyticus*, and *Shigella flexneri* and Gram-

Received: August 17, 2021
Accepted: March 1, 2022
Published: March 15, 2022

positive *S. aureus* and *Bacillus subtilis* with the reported detection limit of 10^5−10^7 CFU/mL.

In order to recognize the bacterial cells, a number of recognition elements including antibodies,[10] aptamers,[11] boronic acid derivatives,[8,12] and vancomycin[13] were used in biosensor development. However, the detecting capability of these recognition elements is often limited to one bacterial species or at best a group of Gram-positive or -negative bacteria. Mannan-binding lectin (MBL) is a protein in blood circulation capable of detecting a broad spectrum of both Gram-positive and -negative bacteria.[14]

MBL is a 25 kDa tulip-shaped protein comprising four domains of a cysteine-rich N-terminal, a collagen-like region, a neck and a C-terminal carbohydrate-recognition domain (CRD).[15,16] MBL is a calcium-dependent protein, recognizing the pathogen-associated molecular patterns (PAMPs) which are conserved molecules present on a variety of microorganisms and playing an essential role in their survival.[17,18] Lipopolysaccharide (LPS) and lipoteichoic acid (LTA) on Gram-negative and -positive bacteria, respectively, are examples of such molecules which induce the host defense response after attachment to MBL and activating the complement system.[19,20]

In this study, MBL was used for the first time as the biorecognition element of the biosensor to detect both Gram-positive and -negative bacteria. The biosensor comprised blue polystyrene microparticles (PSM), as the signal transducer, with the MBL protein chains (MBL-PSM) immobilized on its surface. The biosensor had a binary (all-or-none) response, visible to the naked eye, where the biosensor retained its blue color in the presence of bacterial cells, while shifting from blue to colorless when bacterial cells were not present. Using the developed biosensor, four Gram-negative bacteria including *E. coli*, *P. aeruginosa*, *Acinetobacter baumannii*, and *Klebsiella pneumoniae*, and two Gram-positive bacteria of *E. faecalis* and *S. aureus* were detected in water samples with a concentration as low as $10^{1.5}$ CFU/mL.

MATERIALS AND METHODS

Synthesis of MBL-PSM. Recombinant human MBL protein (Sino Biological, catalogue number 10405-HNAS) was immobilized on the carboxyl-functionalized polystyrene microparticles (PSM; Spherotech, catalogue number CPB-005-10). The step-by-step protocol of the coupling procedure is described in the Supporting Information. In brief, the PSM aliquot in Milli-Q water (18 MΩ/cm resistivity) was centrifuged at 12,000 rpm for 5 min. The supernatant was discarded and the PSM were resuspended in 50 mM MES buffer (Sigma-Aldrich, catalogue number M8902) to make a 5 mg/mL suspension. Next, 1-ethyl-3-(3-(dimethylamino)propyl) carbodiimide hydrochloride (EDC; Thermo Scientific, catalogue number 22980) and *N*-hydroxysulfosuccinimide (Sulfo-NHS; Thermo Scientific, catalogue number 24510) were added to the buffer to make the final concentrations of 1.90 and 12.90 mg/mL, respectively. A freshly dissolved 25 μg of MBL in 50 mM MES buffer (1 mg/mL) was added to 1 mg of PSM and allowed to mix on an orbital shaker at 250 rpm for 2.50 h. Next, ethanolamine (Sigma-Aldrich, catalogue number E9508) was added to the medium and mixed for an additional 30 min on the orbital shaker at 250 rpm. The medium was then centrifuged at 12,000 rpm for 5 min, and the supernatant was collected for bicinchoninic acid (BCA) assay analysis. Finally, the MBL-PSM were resuspended in 200 μL Dulbecco's phosphate-buffered saline (DPBS; Gibco, catalogue number 14190250). The entire process was performed under ambient conditions (relative humidity, 30−70%; temperature, 20 ± 5 °C).

Characterization of the MBL-PSM. *Conductometric Titration.* The density of carboxyl groups on the outer surface of PSM was measured using a titrator (Excellence Titrator T5, Mettler Toledo, Switzerland). The PSM were diluted in Milli-Q water (solid content 0.45%), and the pH was adjusted between 2.50 and 3 using 0.10 M HCl solution. The change in the conductivity of PSM at 23 °C after adding 0.10 M NaOH solution was used to calculate the mean number of carboxyl groups per particle. The detailed calculation can be found in the Supporting Information.

BCA Assay Analysis. BCA assay analysis was carried out to determine the coupling efficiency of MBL protein with the PSM. The supernatant collected at the end of the conjugation process was tested using a Pierce Rapid Gold BCA Protein Assay Kit (Thermo Scientific, catalogue number A53227), following the manufacturer's instructions. In brief, the two reagents available in the kit were mixed shortly before the test and added (100 μL) to 10 μL of the supernatant, as well as a series of bovine serum albumin (BSA; Sigma-Aldrich, catalogue number A2153) solutions (0−2000 μg/mL) in a 96-well plate. The plate then was immediately transferred to a microplate reader (Infinite 200 pro, Tecan, Switzerland) and the absorbance was read at 480 nm after 5 min of shaking at ambient conditions. The absorbance of the supernatant was then compared against the standard curve plotted from the BSA solutions.

Dynamic Light Scattering (DLS). The particle size and charge were measured using a DLS analyzer (NanoBrook Omni, Brookhaven Instruments, USA). The samples (pH 7.40) were transferred to a disposable cuvette and analyzed at 5 automated acquisitions.

Quartz Crystal Microbalance with Dissipation Monitoring (QCM-D). The orientation of MBL protein attached onto the PSM was assessed using the QSense Analyzer (Biolin Scientific, Sweden). The MBL-PSM diluted in Milli-Q water (5 μg/mL) was incubated on a bare gold sensor at 23 °C. After 7 h, the sensor was washed by DPBS at a flow rate of 100 μL/min for 30 min to wash away the unattached particles. The adsorbed mass from the frequency and dissipation shifts was calculated using the built-in viscoelastic model in the software Q-sense Dfind (Biolin Scientific, Sweden).

The MBL-Based Biosensor Testing. The testing was carried out by mixing 25 μL of each sample with 4 μL of the MBL-PSM and 3 μL of 3.40 mM calcium chloride dihydrate (Merck, catalogue number 1023820250) in Milli-Q water. The mixture was then incubated for 20 min under ambient conditions, followed by mixing with 25 μL of 70% (v/v) ethanol in water. The color of medium after 15 min was measured using the microplate reader at 660 nm.

Bacteria Cell Wall Components. LPSs from *E. coli* O128: B12 (Sigma-Aldrich, catalogue number L2755), *P. aeruginosa* (Sigma-Aldrich, catalogue number L9143), and *S. typhimurium* (Sigma-Aldrich, catalogue number L7261) were used as the characteristic components of Gram-negative bacteria cell wall. LTAs from *S. aureus* (Sigma-Aldrich, catalogue number L2515) and *Streptococcus pyogenes* (*S. pyogenes*; Sigma-Aldrich, catalogue number L3140) were used as the components found on the cell wall of Gram-positive bacteria. Each component was mixed with Milli-Q water to prepare four concentrations of 1, 2.50, 5, and 10 ppm. Potable water ($[Ca^{2+}]$ < 7 ppm) from a local water supply was tested as the negative control.

Bacteria Culture. Four Gram-negative bacteria including *Acinetobacter baumanii* (*A. baumanii;* ATCC 17978), *E. coli* (G102, O86:H2), *Klebsiella pneumoniae* (*K. pneumoniae;* ATCC 13883), *P. aeruginosa* (ATCC 27583), and two Gram-positive bacteria *E. faecalis* (ATCC 29212) and *S. aureus* (ATCC 6538) were used in this study. All species were grown on LB agar plates from frozen glycerol stocks except for *S. aureus* which was grown on nutrient agar. A single colony of each bacterium was inoculated in 10 mL of LB broth medium and incubated at 37 °C for 24 h under 200 rpm shaking. The bacteria concentration in the suspension was determined by plating the stock on agar and counting the number of colonies. The suspension was then centrifuged at 12,000 rpm for 5 min, and the bacteria collected were washed with DPBS twice and resuspended in Milli-Q water. The suspension was then decimally diluted in Milli-Q water to achieve the following bacteria concentrations of 10^4, 10^3, 10^2, and 10^1 CFU/mL. The concentrations of the serially diluted suspensions were confirmed by spreading them on agar plates in triplicate and incubating for 24 h before counting the colonies. Potable water ($[Ca^{2+}]$ < 7 ppm) from a local water supply was tested as the negative control.

https://doi.org/10.1021/acssensors.1c01748
ACS Sens. 2022, 7, 951−959

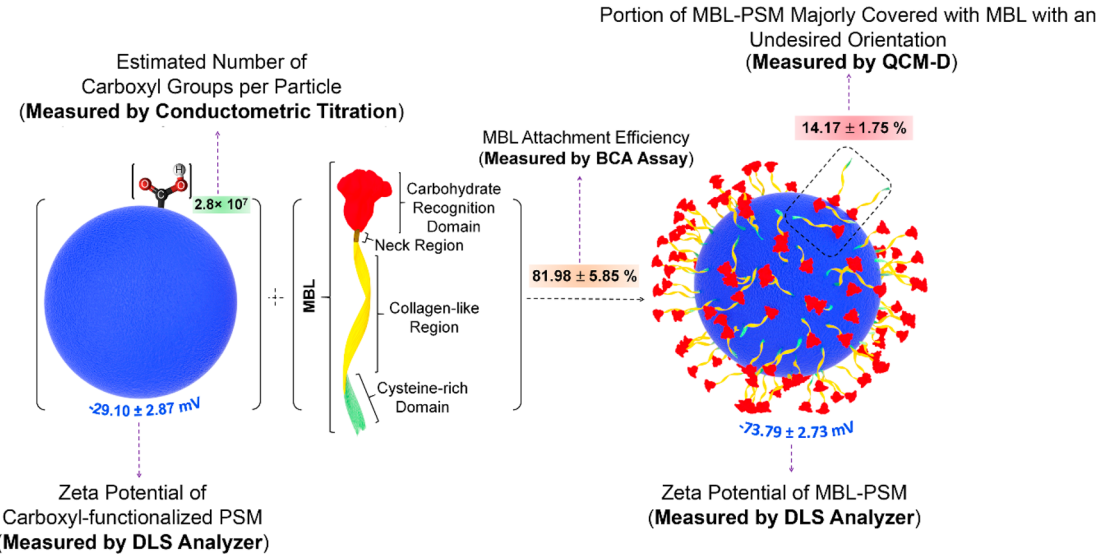

Figure 1. Summary of the characterizations performed on the biosensor herein synthesized. MBL; Mannan-binding lectin, MBL-PSM; Polystyrene microparticles coupled with mannan-binding lectin protein.

Wastewater Samples. The capability of the biosensor to detect pathogens in real-life wastewater was tested against the samples obtained from a paper industry water treatment plant in Victoria, Australia. The analytical data of the water used in this study is found in Table S1. The samples were diluted 100 times with Milli-Q water to adjust the hardness (to ~7 ppm [Ca^{2+}]), and the resultant samples were tested once without further modification and after being autoclaved at 121 °C and filtered (0.20 μm syringe filter).

Statistical Analysis. The obtained results were statistically analyzed using Student's *t*-test by Minitab 17 software (Minitab Inc., USA), and the $p < 0.05$ was considered statistically significant.

RESULTS AND DISCUSSION

Characterization of the Synthesized Biosensor. The conductometric titration, DLS, BCA, and QCM-D analysis were carried out to characterize the synthesized biosensor, with the corresponding results were summarized in Figure 1. The conductometric titration estimated the presence of 2.80×10^7 carboxyl groups per PSM. The MBL protein chains were coupled with the carboxyl groups on the PSM via their amine groups. The BCA analysis revealed that this process ended up attaching 81.98 ± 5.85% of the used MBL to the PSM. The obtained result was further confirmed by DLS analysis. The conjugation of negatively charged MBL[21] significantly ($p < 0.005$) increased the zeta potential of carboxyl-functionalized PSM from −29.10 ± 2.87 mV to −73.79 ± 2.73 mV. Note that the nature of BCA assay, which measures the total protein content, might measure the protein impurities of the commercial MBL used in this study (>95% purity), resulted in estimating a smaller attachment efficiency.[22]

A high attachment efficiency, in addition to its cost benefits, is critical for optimal biosensor performance. The dissociation constant (K_D) of MBL to saccharides is relatively high (10^{-3} M),[23] when compared with the known antibody−antigen interaction (10^{-10} to 10^{-9} M).[24] Hence, a large number of MBL chains must be present on each PSM to potentially enhance the biosensor avidity to the bacteria through simultaneous multiple binding.[25,26] In the serum, MBL enhances its avidity by forming hexamers. The MBL chains first form a triple helix, referred to as "subunit", at the collagen-like region which then link together through the disulfide bridges at their N-termini and form the hexamers.[16]

The orientation of attached MBL chains on microparticles is another critical factor for optimized biosensor functionality. The importance of orientation has been previously demonstrated for the affinity of the antibodies to their antigens.[24] The biorecognition site in the MBL protein resides at its C-terminal which makes the ideal orientation the N-terminal attached to the PSM, while the C-terminal is exposed. Of the 298 amino acids constructing the MBL protein, 7 are cysteine.[19] Out of these 7 cysteine residues, 4 in the C-terminal are capped through the disulfide bonding, while the remaining 3 in the N-terminal domain are exposed.[27] The availability of these free cysteine residues, combined with the high affinity of thiol groups on cysteine to the gold surfaces,[10] were the basis of the QCM-D analysis here. Incubating the MBL-PSM on a gold sensor resulted in the attachment of an estimated 14.17 ± 1.75% of the particles, expected to be the portion of particles mostly covered with MBL with an undesired orientation (i.e., CRD not being available). It is noteworthy that this high percentage can be partially attributed to the water trapped between the MBL chains which could result in an overestimation of the calculated mass.[28] Measuring the hydrodynamic diameter of the MBL-PSM strengthens this hypothesis, as the MBL conjugation significantly ($p < 0.005$) increased the mean hydrodynamic diameter of the bare PSM from 431.25 ± 2.97 nm to 767.84 ± 19.88 nm.

Kang et al.[29] chose a different approach and used engineered MBL with deleted collagen-like region fused to the human IgG1 Fc (FcMBL). Deleting the collagen-like region was done in order to eliminate the blood coagulation activity of this region when MBL came in contact with blood in their blood-cleansing device. However, since the present study dealt with water samples, not blood, wild-type MBL was preferred over FcMBL, as it could only add to the cost and complexity of the synthesis procedure.

Principle of the Assay. Figure 2 illustrates the testing procedure of the colorimetric assay used in this study. The water sample was first mixed with the MBL-PSM and calcium ions and incubated for 20 min to ensure efficient binding between the

https://doi.org/10.1021/acssensors.1c01748
ACS Sens. 2022, 7, 951−959

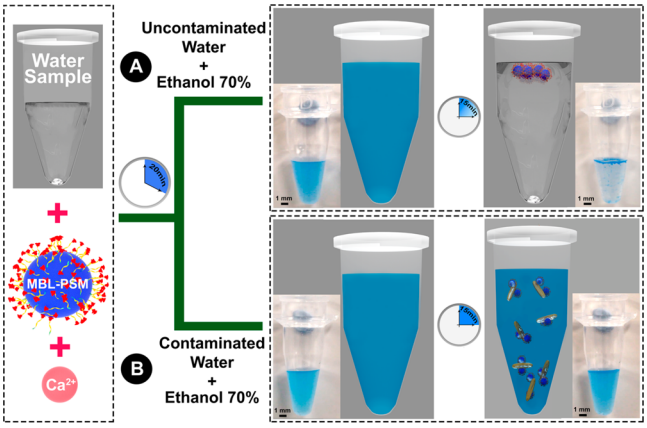

Figure 2. Colorimetric assay procedure of the developed biosensor.

analyte and the biosensor. Next, ethanol was added to the blue mixture and incubated for a further 15 min. A visible color shift from blue to colorless (Figure 2A) occurred as a result of the gradual aggregation and separation of blue particles (Supporting Video 1). This was interpreted as the analyte being absent or existing below the assay's detection limit. On the other hand, if the blue color persisted at 15 min reading time, it was interpreted as the analyte being present in the sample (Figure 2B). Indeed, the aggregation eventually happens even in this sample if it is given extra time (i.e., more than 5 min after the reading time).

The resulting particle aggregation observed after ethanol addition can be explained by two mechanisms. Ethanol, being an organic solvent, decreases the solubility of hydrophilic amino acid-rich proteins such as MBL.[30] Only tryptophan has been shown to have increased solubility after ethanol addition,[31] but since this represents only 1.30% of the total amino acid content of MBL, the effect is negligible. Ethanol also enhances the interaction of calcium ions with MBL-PSM by decreasing the dielectric constant of the medium.[32,33] This was responsible for the further instability of the colloid and its eventual aggregation by the known charge neutralization flocculation mechanism.[34] The zeta potential measurement of the 1 ppm *E. coli*'s LPS sample confirmed this, as the MBL-PSM showed a rapid decrease in the net charge from −73.79 ± 2.73 mV to about −6 mV after 10 min. When the particles came together, it is expected that they attach to each other by entangling their MBL protein chains. Such an entanglement is possible given the sufficiently long length of each MBL chain which on average reaches 19 ± 4 nm.[21] To put this in perspective, the MBL chain length is almost three times longer than the length of a typical IgG antibody.[35]

MBL, as the recognition agent of the biosensor, identifies the microbial saccharides including *N*-acetyl-D-glucosamine, mannose, *N*-acetyl-mannosamine, and fucose and binds to their 3- and 4-hydroxyl groups.[26,36] It is hypothesized that when the bacterial cells or the cell-wall components were present, they attached to multiple MBL-PSM and created particle clusters by interparticle bridging. Considering the relatively large size of monomeric LPS and LTA, which can form spherical assemblies with tens of nanometers in diameter[37,38] and their tendency to self-assemble and grow in size up to 1 μm,[39] this assumption is reasonable. The DLS measurement confirmed this hypothesis as the incubation of MBL-PSM with 2.50 ppm LPS of *E. coli* resulted in an increase in the average particle size up to 2341 ± 217 nm and the polydispersity index from 0.20 ± 0.06 to 0.50 ± 0.02 after 20 min. The clusters formed at this stage (Figure S1A) were different from the aggregates observed in the uncontaminated sample (Figure S1B) after ethanol addition. These clusters, despite their large size (∼2 μm), were still homogeneously dispersed in the medium, yielding a blue color. It can also be hypothesized that when ethanol was added, the conformation of MBL changed by altering the hydrogen bonding properties of the aqueous medium.[40,41] As a result, when the free MBL-PSM started to self-aggregate, the LPS/LTA-MBL-PSM clusters began to disintegrate, releasing the dissociated particles into the medium.[40] The released particles counter-balanced the effect of self-aggregation, extending the intensity of the blue color in the contaminated sample for a longer time. Similar dissociation behavior has been previously observed when antibodies came in contact with ethanol,[41] high ionic strength medium,[42] and acids.[43]

Detecting the Bacteria PAMPs. To find the optimal incubation time by which MBL-PSM were aggregated after ethanol addition, LPS and LTA, as the respective characteristic components of Gram-negative and-positive bacteria cell walls, were used. LPS (endotoxin) makes up about 75% of the outer membrane of Gram-negative bacteria.[44] It is anchored to the bacteria membrane through a glycophospholipid domain called "lipid A" which itself is attached to a core oligosaccharide and a distal polysaccharide known as "O-antigen".[45,46] Teichoic acids (TAs) are the constituent of about 50% of the membrane in Gram-positive bacteria.[47] They are found covalently linked to the cell wall peptidoglycan as wall teichoic acid (WTA)[48] or tethered to the cell membrane (LTA).[49] Wall teichoic acid has also been demonstrated to be more diverse structurally, while LTA often is less diverse among bacterial species.[50] LTA makes up about 10% of the Gram-positive bacteria membrane and is made up of phosphate-linked repeating units of alcohols such as glycerol or ribitol anchored to the membrane by glycolipid domain.[49,51]

The MBL−PAMPs interaction *in vitro* is reported to require 20 min to establish proper binding under ambient conditions.[14,52,53] Our experiments verified this number (Figure S2), and thus all samples were incubated with the MBL-PSM and $CaCl_2$ for 20 min prior to mixing with ethanol. After ethanol addition, the color intensities of samples were measured at 660 nm after 5, 10, and 15 min, and the results were shown in Figure 3. It was found that an absorbance of 0.10 was the value below which the samples changed their color from visibly blue to colorless, as judged by the naked eye. Potable water and the sucrose in Milli-Q water (10 ppm) reached the 0.10 limit 15 min after ethanol addition. As MBL recognizes the saccharide moieties on bacteria, sucrose in the concentration of 10 ppm was included to verify that the biosensor does not generate false-positive results when tested against the non-microbial saccharides. Next, the LPS from *E. coli*, *P. aeruginosa*, and *S. typhimurium* and LTA from *S. aureus* and *S. pyogenes* were added to the Milli-Q water to prepare four concentrations of 1, 2.50, 5, and 10 ppm. All tested PAMPs at 2.50, 5, and 10 ppm were visibly blue after 15 min, while the measured absorbance for all 1 ppm samples dropped below the 0.10 blue/colorless borderline absorbance.

The decreased analytical sensitivity of the biosensor in detecting the PAMPs when compared with the previously developed biosensors[54−56] can be attributed to the nature of PAMPs tested in this study. The MBL ligand for *E. coli* is lipid A residue of its LPS,[57] while the ligands for *S. aureus*[50,51] and *S. pyogenes*[58,59] are the *N*-acetylglucosamine of their WTA. The commercial LPS used here has been extracted via the phenol

https://doi.org/10.1021/acssensors.1c01748
ACS Sens. 2022, 7, 951−959

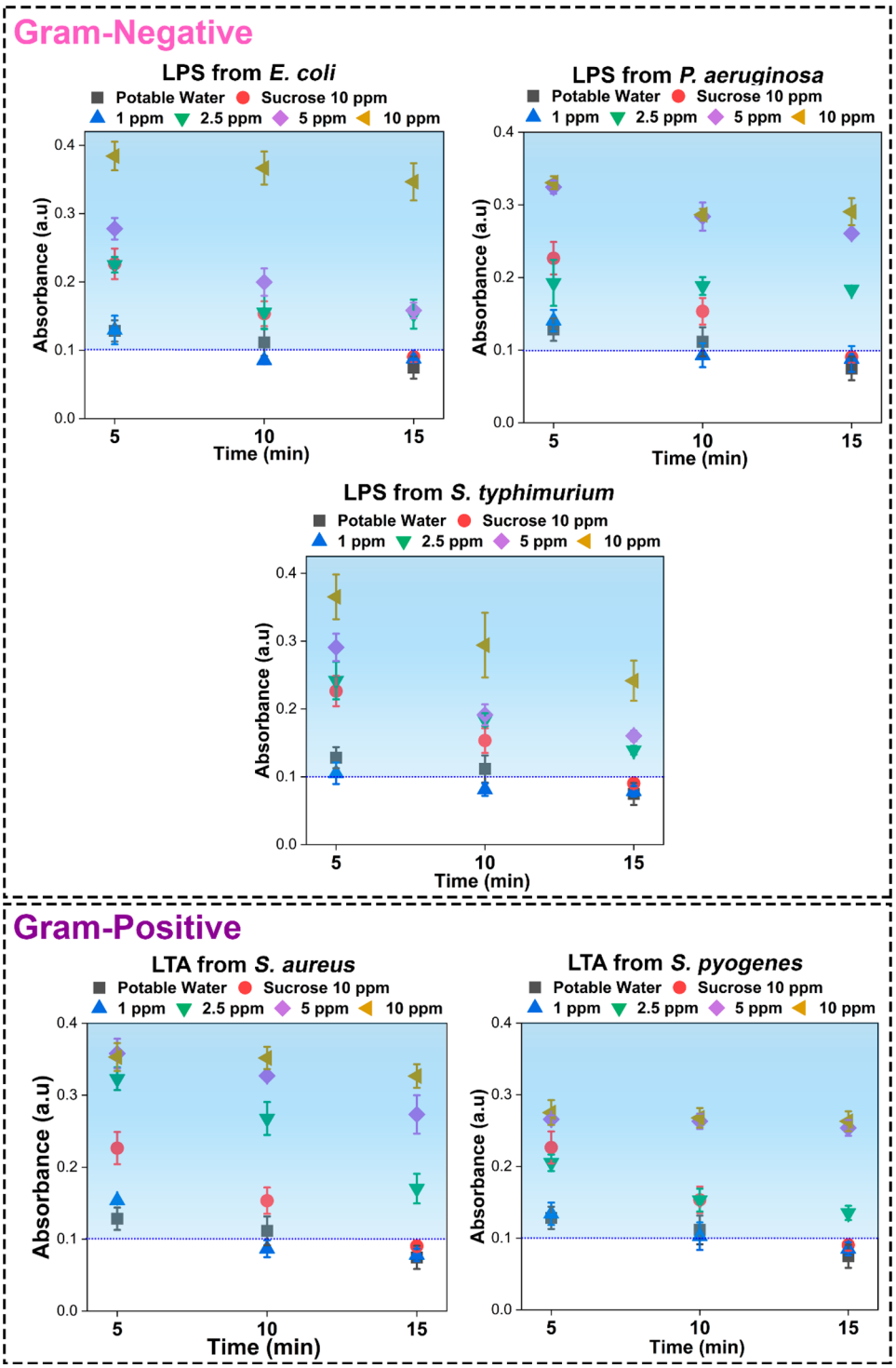

Figure 3. Color changing behavior of the biosensor 5, 10, and 15 min after ethanol addition measured by a microplate reader at 660 nm. The 0.10 was the absorbance value below which the samples shifted color from visibly blue to colorless. LPS; Lipopolysaccharide, LTA; Lipoteichoic acid.

extraction method. It has been demonstrated that this technique generates LPS with about 60% of its original lipid A content.[60] Additionally, as the main ligand of MBL on *S. aureus* and *S. pyogenes* resides on their WTA, measuring LTA which is considered a poor ligand for MBL in these bacteria[61] resulted in having a lower analytical sensitivity. Another example is *S. typhimurium* whose MBL ligand resides on the core oligosaccharide of its LPS, but the attached O-antigen diminished its interaction with the MBL CRD.[26] It has been recommended that the LPS level in potable water supply must not exceed 0.10 ppm, as it can have adverse health effects.[62] The LPS level in the effluent from water treatment plants is usually much lower than this amount.[39] This makes the developed biosensor unsuitable for the measurement of free PAMPs, as it was designed for the detection of whole bacterial cells.

Detecting Gram-Positive and -Negative Bacterial Cells. Figure 4 illustrates the performance of developed biosensor detecting four Gram-negative (i.e., *E. coli*, *P.*

https://doi.org/10.1021/acssensors.1c01748
ACS Sens. 2022, 7, 951−959

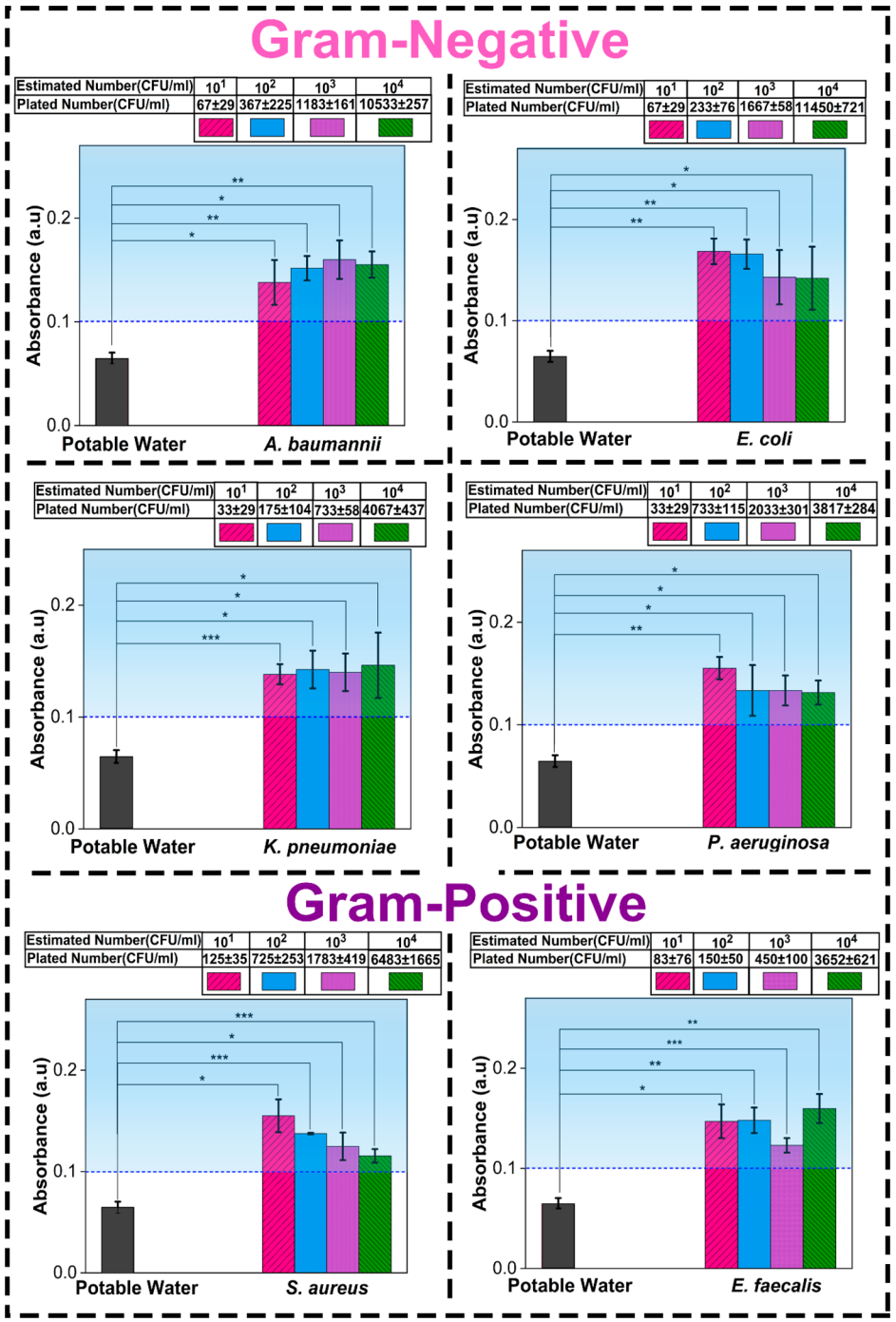

Figure 4. Color changing behavior of the biosensor in water samples spiked with 10^1−10^4 CFU/mL of Gram-positive and -negative bacteria vs potable water measured by a microplate reader at 660 nm. The 0.10 was the absorbance value below which the samples shifted color from visibly blue to colorless. Values represent the mean ± standard deviation, $n = 3$, $^*p < 0.05$, $^{**}p < 0.01$, $^{***}p < 0.005$ (obtained by Student's *t*-test).

aeruginosa, *K. pneumoniae*, and *A. baumannii*) and two Gram-positive (i.e., *S. aureus* and *E. faecalis*) bacteria. The measured blue color intensity for all six species in all four estimated concentrations of 10^1, 10^2, 10^3, and 10^4 CFU/mL were above the 0.10 blue/colorless borderline (the optical images were shown in Figure S3). The blue color intensities in all contaminated samples were significantly greater than that of the potable water. However, no statistically significant differences were observed among different concentrations of each bacterium, indicating the intensity of blue color was not influenced by the bacteria concentration tested. It is worth mentioning that despite achieving a higher analytical sensitivity compared with the previous studies,[7−9] the developed biosensor still is not suitable for water safety standard testing. According to the United States Environmental Protection Agency (EPA), the analytical sensitivity of a test for determining the safety of potable water must be at least 1 CFU/100 mL.[63]

The colony production is a distinctive feature of live bacteria, which separates them from dead, nonviable, or resting-state ones.[64] Regardless of this unique feature, the chemical composition of live bacteria is not significantly different from the rest.[65] This theoretically makes it possible to detect them, as

https://doi.org/10.1021/acssensors.1c01748
ACS Sens. 2022, 7, 951−959

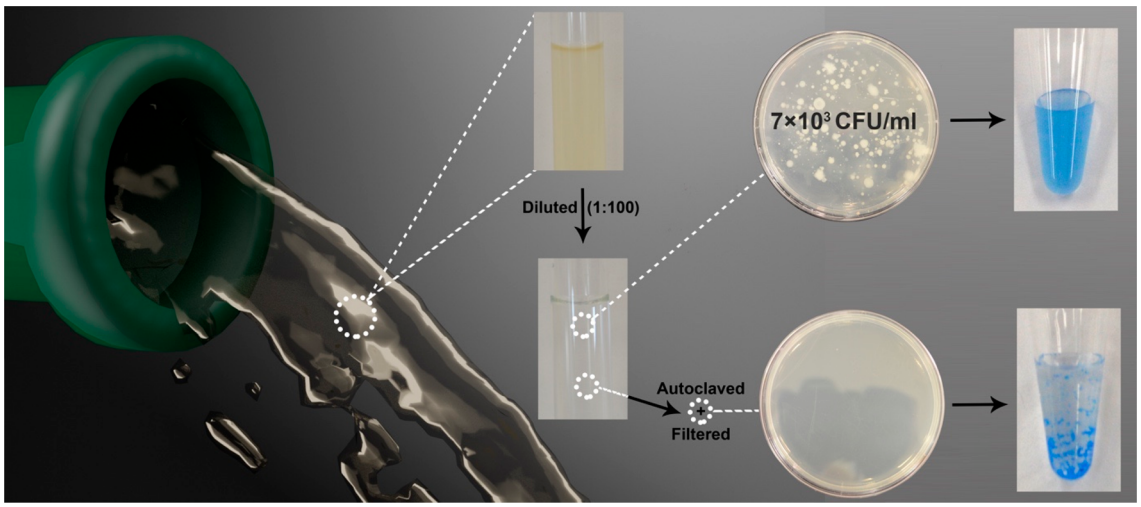

Figure 5. Biosensor performance tested on the wastewater samples. The sample was diluted 100 times and tested without further treatment and after autoclave/filtering.

well as those which are dead, nonviable, or in a resting state using the developed biosensor. A possible explanation for its capability in detecting low levels of CFU partially relies on the presence of such cells, in addition to the live ones.[66]

Wastewater Samples from the Water Treatment Plant. Testing the water samples obtained from a water treatment plant confirmed the feasibility of detecting the bacterial cells in this type of water. As Figure 5 shows, the biosensor/sample medium retained its blue color when bacteria were present and lost its color in their absence. Due to the high water hardness, the sample was diluted 100 times to decrease the calcium ion concentration. It was observed that a very high calcium content could aggregate the MBL-PSM regardless of bacteria presence or absence even before the ethanol addition. This phenomenon was observed when the calcium concentration in both wastewater and potable water was above 7 ppm. Below this concentration, no change in the biosensor performance discernible by the naked eye was observed.

CONCLUSION

The present study reports the development of a visual biosensor capable of detecting Gram-positive and -negative bacteria in water samples. The biosensor provided a culture-free, rapid, and on-site detection, detecting the bacteria at concentrations as low as $10^{1.50}$ CFU/mL.This makes the current biosensor at least 10 times more sensitive than the visual biosensors with similar functionality reported in the literature. Testing the biosensor on wastewater demonstrated its capability to detect bacteria in real-life samples. However, it was found that the performance could be compromised when testing the water samples with high ionic concentrations.

ASSOCIATED CONTENT

Supporting Information

The Supporting Information is available free of charge at https://pubs.acs.org/doi/10.1021/acssensors.1c01748.

The step-by-step protocol of MBL attachment to PSM; calculation of the mean number of carboxyl groups per particle; wastewater sample analytical data; scanning electron microscopy images of the MBL-PSM; required time to establish a proper binding between MBL and PAMPs; and optical images of the bacterial cell containing samples 15 min after ethanol addition (PDF)

Color changing behavior of biosensor (MBL-conjugated blue microparticles) when testing the contaminated and potable water. The biosensor was first added to each sample and incubated for 20 min. Next, ethanol 70% (v/v) was added to the mixture and the color change was observed after 15 min. A visible color shift from blue to colorless occurred in the potable water while contaminated water remained blue. (MP4)

AUTHOR INFORMATION

Corresponding Author

Warren Batchelor − *Bioresource Processing Research Institute of Australia (BioPRIA), Department of Chemical Engineering, Monash University, Clayton, Victoria 3800, Australia;* orcid.org/0000-0001-6880-7765; Email: Warren.batchelor@monash.edu

Authors

Mahdi Naseri − *Bioresource Processing Research Institute of Australia (BioPRIA), Department of Chemical Engineering, Monash University, Clayton, Victoria 3800, Australia;* orcid.org/0000-0001-5572-5189

Maisha Maliha − *Bioresource Processing Research Institute of Australia (BioPRIA), Department of Chemical Engineering, Monash University, Clayton, Victoria 3800, Australia*

Mostafa Dehghani − *Bioresource Processing Research Institute of Australia (BioPRIA), Department of Chemical Engineering, Monash University, Clayton, Victoria 3800, Australia;* orcid.org/0000-0001-5019-725X

George P Simon − *Department of Materials Science and Engineering, Monash University, Clayton, Victoria 3800, Australia*

Complete contact information is available at: https://pubs.acs.org/10.1021/acssensors.1c01748

Notes

The authors declare no competing financial interest.

https://doi.org/10.1021/acssensors.1c01748
ACS Sens. 2022, 7, 951−959

■ ACKNOWLEDGMENTS

The authors are grateful for the financial support from the Chemical Engineering Department of Monash University, Bioresource Processing Research Institute of Australia (BioPRIA), and the scholarship given to M. Naseri by the Australian Government Research Training Program (RTP). The authors also express their gratitude to Stefan Buergmayr and Rajini Brammananth for providing the wastewater samples and frozen bacterial stocks, respectively. The help from Dr. Vikram Singh Raghuwanshi and Laila Hossain in conducting the QCM-D and conductometric titration analysis, respectively, is also appreciated. The authors acknowledge the use of the facilities at Monash Institute of Medical Engineering (MIME) and Monash Centre for Electron Microscopy, a Node of Microscopy Australia.

■ REFERENCES

(1) Saylan, Y.; Erdem, Ö.; Cihangir, N.; Denizli, A. Detecting fingerprints of waterborne bacteria on a sensor. *Chemosensors* **2019**, *7* (3), 33.
(2) Kumar, N.; Hu, Y.; Singh, S.; Mizaikoff, B. Emerging biosensor platforms for the assessment of water-borne pathogens. *Analyst* **2018**, *143* (2), 359−373.
(3) McLeod, J.; Park, C.; Cunningham, A.; O'Donnell, L.; Brown, R. S.; Kelly, F.; She, Z. Developing a toll-like receptor biosensor for Gram-positive bacterial detection and its storage strategies. *Analyst* **2020**, *145* (18), 6024−6031.
(4) Bhardwaj, N.; Bhardwaj, S. K.; Bhatt, D.; Lim, D. K.; Kim, K.-H.; Deep, A. Optical detection of waterborne pathogens using nanomaterials. *TrAC, Trends Anal. Chem.* **2019**, *113*, 280−300.
(5) Yaghoubi, M.; Rahimi, F.; Negahdari, B.; Rezayan, A. H.; Shafiekhani, A. A lectin-coupled porous silicon-based biosensor: label-free optical detection of bacteria in a real-time mode. *Sci. Rep* **2020**, *10* (1), 1−12.
(6) Alhadrami, H. A. Biosensors: Classifications, medical applications, and future prospective. *Biotechnol. Appl. Biochem* **2018**, *65* (3), 497−508.
(7) Sun, J.; Huang, J.; Li, Y.; Lv, J.; Ding, X. A simple and rapid colorimetric bacteria detection method based on bacterial inhibition of glucose oxidase-catalyzed reaction. *Talanta* **2019**, *197*, 304−309.
(8) Huang, J.; Sun, J.; Warden, A. R.; Ding, X. Colorimetric and photographic detection of bacteria in drinking water by using 4-mercaptophenylboronic acid functionalized AuNPs. *Food Control* **2020**, *108*, 106885.
(9) Du, J.; Yu, Z.; Hu, Z.; Chen, J.; Zhao, J.; Bai, Y. A low pH-based rapid and direct colorimetric sensing of bacteria using unmodified gold nanoparticles. *J. Microbiol. Methods* **2021**, *180*, 106110.
(10) Bui, M.-P. N.; Ahmed, S.; Abbas, A. Single-digit pathogen and attomolar detection with the naked eye using liposome-amplified plasmonic immunoassay. *Nano Lett.* **2015**, *15* (9), 6239−6246.
(11) Jin, B.; Yang, Y.; He, R.; Park, Y. I.; Lee, A.; Bai, D.; Li, F.; Lu, T. J.; Xu, F.; Lin, M. Lateral flow aptamer assay integrated smartphone-based portable device for simultaneous detection of multiple targets using upconversion nanoparticles. *Sens. Actuators, B* **2018**, *276*, 48−56.
(12) Zheng, L.; Qi, P.; Zhang, D. A simple, rapid and cost-effective colorimetric assay based on the 4-mercaptophenylboronic acid functionalized silver nanoparticles for bacteria monitoring. *Sens. Actuators, B* **2018**, *260*, 983−989.
(13) You, Q.; Zhang, X.; Wu, F.-G.; Chen, Y. Colorimetric and test stripe-based assay of bacteria by using vancomycin-modified gold nanoparticles. *Sens. Actuators, B* **2019**, *281*, 408−414.
(14) Cartwright, M.; Rottman, M.; Shapiro, N. I.; Seiler, B.; Lombardo, P.; Gamini, N.; Tomolonis, J.; Watters, A. L.; Waterhouse, A.; Leslie, D. A broad-spectrum infection diagnostic that detects pathogen-associated molecular patterns (PAMPs) in whole blood. *EBioMedicine* **2016**, *9*, 217−227.
(15) Wang, M.; Zhang, Y.; Chen, Y.; Zhang, L.; Lu, X.; Chen, Z. Mannan-binding lectin regulates dendritic cell maturation and cytokine production induced by lipopolysaccharide. *BMC Immunol* **2011**, *12* (1), 1−10.
(16) Arnold, J. N.; Dwek, R. A.; Rudd, P. M.; Sim, R. B. Mannan binding lectin and its interaction with immunoglobulins in health and in disease. *Immunol. Lett.* **2006**, *106* (2), 103−110.
(17) Kasperkiewicz, K.; Swierzko, A. S.; Bartlomiejczyk, M. A.; Cedzynski, M.; Noszczynska, M.; Duda, K. A.; Michalski, M.; Skurnik, M. Interaction of human mannose-binding lectin (MBL) with Yersinia enterocolitica lipopolysaccharide. *Int. J. Med. Microbiol* **2015**, *305* (6), 544−552.
(18) Zipfel, C.; Robatzek, S. Pathogen-associated molecular pattern-triggered immunity: veni, vidi···? *Plant Physiol* **2010**, *154* (2), 551−554.
(19) Garred, P.; Larsen, F.; Seyfarth, J.; Fujita, R.; Madsen, H. O. Mannose-binding lectin and its genetic variants. *Genes Immun* **2006**, *7* (2), 85−94.
(20) Cao, Y.; Naseri, M.; He, Y.; Xu, C.; Walsh, L. J.; Ziora, Z. M. Non-antibiotic antimicrobial agents to combat biofilm-forming bacteria. *J. Glob. Antimicrob. Resist* **2020**, *21*, 445−451.
(21) Jensenius, H.; Klein, D. C.; van Hecke, M.; Oosterkamp, T. H.; Schmidt, T.; Jensenius, J. C. Mannan-binding lectin: structure, oligomerization, and flexibility studied by atomic force microscopy. *J. Mol. Biol.* **2009**, *391* (1), 246−259.
(22) Worsley, G. J.; Kumarswami, N.; Minelli, C.; Noble, J. E. Characterisation of antibody conjugated particles and their influence on diagnostic assay response. *Anal. Methods* **2015**, *7* (22), 9596−9603.
(23) Jack, D. L.; Klein, N. J.; Turner, M. W. Mannose-binding lectin: targeting the microbial world for complement attack and opsonophagocytosis. *Immunol. Rev.* **2001**, *180* (1), 86−99.
(24) Tajima, N.; Takai, M.; Ishihara, K. Significance of antibody orientation unraveled: well-oriented antibodies recorded high binding affinity. *Anal. Chem.* **2011**, *83* (6), 1969−1976.
(25) Arnold, J. N.; Wormald, M. R.; Suter, D. M.; Radcliffe, C. M.; Harvey, D. J.; Dwek, R. A.; Rudd, P. M.; Sim, R. B. Human serum IgM glycosylation identification of glycoforms that can bind to mannan-binding lectin. *J. Biol. Chem.* **2005**, *280* (32), 29080−29087.
(26) Devyatyarova-Johnson, M.; Rees, I. H.; Robertson, B. D.; Turner, M. W.; Klein, N. J.; Jack, D. L. The Lipopolysaccharide Structures of Salmonella enterica Serovar Typhimurium and Neisseria gonorrhoeae-Determine the Attachment of Human Mannose-Binding Lectin to Intact Organisms. *Infect. Immun.* **2000**, *68* (7), 3894−3899.
(27) Wallis, R. Interactions between mannose-binding lectin and MASPs during complement activation by the lectin pathway. *Immunobiology* **2007**, *212* (4−5), 289−299.
(28) Boujday, S.; Bantegnie, A.; Briand, E.; Marnet, P.-G.; Salmain, M.; Pradier, C.-M. In-depth investigation of protein adsorption on gold surfaces: correlating the structure and density to the efficiency of the sensing layer. *J. Phys. Chem. B* **2008**, *112* (21), 6708−6715.
(29) Kang, J. H.; Super, M.; Yung, C. W.; Cooper, R. M.; Domansky, K.; Graveline, A. R.; Mammoto, T.; Berthet, J. B.; Tobin, H.; Cartwright, M. J. An extracorporeal blood-cleansing device for sepsis therapy. *Nature medicine* **2014**, *20* (10), 1211.
(30) Nick Pace, C.; Trevino, S.; Prabhakaran, E.; Martin Scholtz, J. Protein structure, stability and solubility in water and other solvents. *Philos. Trans. R. Soc. B* **2004**, *359* (1448), 1225−1235.
(31) Yoshikawa, H.; Hirano, A.; Arakawa, T.; Shiraki, K. Mechanistic insights into protein precipitation by alcohol. *Int. J. Biol. Macromol.* **2012**, *50* (3), 865−871.
(32) Kleemann, C.; Zink, J.; Selmer, I.; Smirnova, I.; Kulozik, U. Effect of Ethanol on the Textural Properties of Whey Protein and Egg White Protein Hydrogels during Water-Ethanol Solvent Exchange. *Molecules* **2020**, *25* (19), 4417.
(33) Van Oss, C. On the mechanism of the cold ethanol precipitation method of plasma protein fractionation. *J. Protein Chem.* **1989**, *8* (5), 661−668.
(34) Singh, P.; Gupta, R.; Choudhary, M.; Pinnaka, A. K.; Kumar, R.; Bhalla, V. Drug and nanoparticle mediated rapid naked eye water test for pathogens detection. *Sens. Actuators, B* **2018**, *262*, 603−610.

(35) Tan, Y. H.; Liu, M.; Nolting, B.; Go, J. G.; Gervay-Hague, J.; Liu, G.-y. A nanoengineering approach for investigation and regulation of protein immobilization. *ACS Nano* **2008**, *2* (11), 2374−2384.
(36) Turner, M. W. The role of mannose-binding lectin in health and disease. *Molecular immunology* **2003**, *40* (7), 423−429.
(37) Santos, N. C.; Silva, A. C.; Castanho, M. A.; Martins-Silva, J.; Saldanha, C. Evaluation of lipopolysaccharide aggregation by light scattering spectroscopy. *Chembiochem* **2003**, *4* (1), 96−100.
(38) LABISCHINSKI, H.; NAUMANN, D.; FISCHER, W. Small and medium-angle X-ray analysis of bacterial lipoteichoic acid phase structure. *European journal of biochemistry* **1991**, *202* (3), 1269−1274.
(39) Zhang, C.; Tian, F.; Zhang, M.; Zhang, Z.; Bai, M.; Guo, G.; Zheng, W.; Wang, Q.; Shi, Y.; Wang, L. Endotoxin contamination, a potentially important inflammation factor in water and wastewater: A review. *Sci. Total Environ.* **2019**, *681*, 365−378.
(40) Bull, H. B.; Breese, K. Interaction of alcohols with proteins. *Biopolymers* **1978**, *17* (9), 2121−2131.
(41) Rehan, M.; Younus, H. Effect of organic solvents on the conformation and interaction of catalase and anticatalase antibodies. *Int. J. Biol. Macromol.* **2006**, *38* (3), 289−295.
(42) Zhang, J.; Sun, Y.; Xu, B.; Zhang, H.; Gao, Y.; Zhang, H.; Song, D. A novel surface plasmon resonance biosensor based on graphene oxide decorated with gold nanorod−antibody conjugates for determination of transferrin. *Biosens. Bioelectron* **2013**, *45*, 230−236.
(43) Pei, R.; Cui, X.; Yang, X.; Wang, E. Real-time immunoassay of antibody activity in serum by surface plasmon resonance biosensor. *Talanta* **2000**, *53* (3), 481−488.
(44) Ramachandran, G. Gram-positive and gram-negative bacterial toxins in sepsis: a brief review. *Virulence* **2014**, *5* (1), 213−218.
(45) Man-Kupisinska, A.; Swierzko, A. S.; Maciejewska, A.; Hoc, M.; Rozalski, A.; Siwinska, M.; Lugowski, C.; Cedzynski, M.; Lukasiewicz, J. Interaction of mannose-binding lectin with lipopolysaccharide outer core region and its biological consequences. *Front. Immunol* **2018**, *9*, 1498.
(46) Lin, I.-H.; Miller, D. S.; Bertics, P. J.; Murphy, C. J.; De Pablo, J. J.; Abbott, N. L. Endotoxin-induced structural transformations in liquid crystalline droplets. *Science* **2011**, *332* (6035), 1297−1300.
(47) Rice, K. C.; Bayles, K. W. Molecular control of bacterial death and lysis. *Microbiol. Mol. Biol. Rev.* **2008**, *72* (1), 85−109.
(48) Schirner, K.; Marles-Wright, J.; Lewis, R. J.; Errington, J. Distinct and essential morphogenic functions for wall-and lipo-teichoic acids in Bacillus subtilis. *EMBO J.* **2009**, *28* (7), 830−842.
(49) Wörmann, M. E.; Corrigan, R. M.; Simpson, P. J.; Matthews, S. J.; Gründling, A. Enzymatic activities and functional interdependencies of Bacillus subtilis lipoteichoic acid synthesis enzymes. *Mol. Microbiol.* **2011**, *79* (3), 566−583.
(50) Xia, G.; Kohler, T.; Peschel, A. The wall teichoic acid and lipoteichoic acid polymers of Staphylococcus aureus. *Int. J. Med. Microbiol* **2010**, *300* (2−3), 148−154.
(51) Nadesalingam, J.; Dodds, A. W.; Reid, K. B.; Palaniyar, N. Mannose-binding lectin recognizes peptidoglycan via the N-acetyl glucosamine moiety, and inhibits ligand-induced proinflammatory effect and promotes chemokine production by macrophages. *J. Immunol* **2005**, *175* (3), 1785−1794.
(52) Kang, J. H.; Super, M.; Yung, C. W.; Cooper, R. M.; Domansky, K.; Graveline, A. R.; Mammoto, T.; Berthet, J. B.; Tobin, H.; Cartwright, M. J. An extracorporeal blood-cleansing device for sepsis therapy. *Nat. Med.* **2014**, *20* (10), 1211.
(53) Bicart-See, A.; Rottman, M.; Cartwright, M.; Seiler, B.; Gamini, N.; Rodas, M.; Penary, M.; Giordano, G.; Oswald, E.; Super, M. Rapid isolation of Staphylococcus aureus pathogens from infected clinical samples using magnetic beads coated with Fc-mannose binding lectin. *PLoS One* **2016**, *11* (6), No. e0156287.
(54) Zhu, L.; Li, S.; Shao, X.; Feng, Y.; Xie, P.; Luo, Y.; Huang, K.; Xu, W. Colorimetric detection and typing of E. coli lipopolysaccharides based on a dual aptamer-functionalized gold nanoparticle probe. *Microchim. Acta* **2019**, *186* (2), 111.
(55) Schenk, F.; Weber, P.; Vogler, J.; Hecht, L.; Dietzel, A.; Gauglitz, G. Development of a paper-based lateral flow immunoassay for simultaneous detection of lipopolysaccharides of Salmonella serovars. *Anal. Bioanal. Chem.* **2018**, *410* (3), 863−868.
(56) Xu, W.; Tian, J.; Shao, X.; Zhu, L.; Huang, K.; Luo, Y. A rapid and visual aptasensor for Lipopolysaccharides detection based on the bulb-like triplex turn-on switch coupled with HCR-HRP nanostructures. *Biosens. Bioelectron* **2017**, *89*, 795−801.
(57) Shiratsuchi, A.; Watanabe, I.; Ju, J. S.; Lee, B. L.; Nakanishi, Y. Bridging effect of recombinant human mannose-binding lectin in macrophage phagocytosis of Escherichia coli. *Immunology* **2008**, *124* (4), 575−583.
(58) Bleiweis, A.; Craig, R.; Coleman, S.; Van de Rijn, I. The streptococcal cell wall: structure, antigenic composition, and reactivity with lysozyme. *J. Dent. Res.* **1971**, *50* (5), 1118−1129.
(59) Schafranski, M. D.; Ferrari, L. P.; Scherner, D.; Torres, R.; Jensenius, J. C.; de Messias-Reason, I. J. High-producing MBL2 genotypes increase the risk of acute and chronic carditis in patients with history of rheumatic fever. *Mol. Immunol* **2008**, *45* (14), 3827−3831.
(60) Barker, J. H.; Kaufman, J. W.; Zhang, D.-S.; Weiss, J. P. Metabolic labeling to characterize the overall composition of Francisella lipid A and LPS grown in broth and in human phagocytes. *Innate Immun* **2014**, *20* (1), 88−103.
(61) Polotsky, V. Y.; Fischer, W.; Ezekowitz, R.; Joiner, K. A. Interactions of human mannose-binding protein with lipoteichoic acids. *Infect. Immun.* **1996**, *64* (1), 380−383.
(62) Anderson, W. B.; George Dixon, D.; Mayfield, C. I. Estimation of endotoxin inhalation from shower and humidifier exposure reveals potential risk to human health. *J. Water Health* **2007**, *5* (4), 553−572.
(63) Tok, S.; de Haan, K.; Tseng, D.; Usanmaz, C. F.; Koydemir, H. C.; Ozcan, A. Early detection of E. coli and total coliform using an automated, colorimetric and fluorometric fiber optics-based device. *Lab Chip* **2019**, *19* (17), 2925−2935.
(64) Barbau-Piednoir, E.; Mahillon, J.; Pillyser, J.; Coucke, W.; Roosens, N. H.; Botteldoorn, N. Evaluation of viability-qPCR detection system on viable and dead Salmonella serovar Enteritidis. *J. Microbiol. Methods* **2014**, *103*, 131−137.
(65) Zhou, H.; Yang, D.; Ivleva, N. P.; Mircescu, N. E.; Schubert, S. r.; Niessner, R.; Wieser, A.; Haisch, C. Label-free in situ discrimination of live and dead bacteria by surface-enhanced Raman scattering. *Anal. Chem.* **2015**, *87* (13), 6553−6561.
(66) Van Nevel, S.; Koetzsch, S.; Proctor, C. R.; Besmer, M. D.; Prest, E. I.; Vrouwenvelder, J. S.; Knezev, A.; Boon, N.; Hammes, F. Flow cytometric bacterial cell counts challenge conventional heterotrophic plate counts for routine microbiological drinking water monitoring. *Water Res.* **2017**, *113*, 191−206.

https://doi.org/10.1021/acssensors.1c01748
ACS Sens. 2022, 7, 951−959